IOP Conf. Series: Materials Science and Engineering **218** (2017) 012012 doi:10.1088/1757-899X/218/1/012012

Spark Plasma Sintering of high-strength ultrafine-grained tungsten carbide

A V Nokhrin[1], V N Chuvil'deev[1], Yu V Blagoveshchenskiy[1], M S Boldin[1], N V Sakharov[1], N V Isaeva[2], A A Popov[1], E A Lantcev[1], O A Belkin[1] and E S Smirnova[1]

[1] Lobachevsky State University of Nizhny Novgorod, 23 Gagarin Ave., Nizhny Novgorod, 603950, Russia.
[2] A.A. Baykov Institute of Metallurgy and Material Science of RAS, 49 Leninsky Ave., Moscow, 119991, Russia

E-mail: nokhrin@nifti.unn.ru

Abstract. The paper dwells on the research conducted into high-rate consolidation of pure tungsten carbide nanopowders using the Spark Plasma Sintering. Studies included the effect that the original size of WC nanoparticles and their preparation modes have on density, structure parameters, and mechanical properties of tungsten carbide. It has been found that materials that show abnormal grain growth during sintering have lower values of sintering activation energy as compared to materials the structure of which is more stable during high-rate heating. A qualitative model is proposed that explains this effect through the dependence of the grain boundary diffusion coefficient on the grain boundary migration rate.

1. Introduction

Pure tungsten carbide is of interest for a variety of applications (cutting tools, drawing dies, etc.) due to a good combination of physical and mechanical properties (high melting temperature, high hardness, low friction coefficient, and chemical resistance to corrosion and oxidation). However, high brittleness of tungsten carbide traditionally obtained with the help of a powder sintering technology does not allow to use it in its purest form. That is why the issue of achieving high mechanical properties with pure tungsten carbide is crucial.

Improving the mechanical properties of tungsten carbide is primarily associated with obtaining ultrafine grains (UFG) in the sintered material [1-2]. To this end, WC nanopowders are used as a initial material. DC arc plasma synthesis is the most advanced method for obtained of WC nanopowders [3, 4].

The Spark Plasma Sintering (SPS) is considered an advanced method applied to obtain materials with high-density UFG structure [5-8]. The core of the SPS lies in the high-rate heating of powder materials in vacuum or inert atmosphere by passing direct pulse large currents through the tooling and samples and simultaneous pressure application. High heating rates become particularly relevant during sintering of UFG materials as they limit the growth of nano- and ultra-dispersed powders and contribute to the formation of a uniform high-density UFG structure at low consolidation temperatures [6-8].

The goal of this paper is to study the structure and properties of tungsten carbide obtained through SPS from nanopowders produced using DC arc plasma synthesis.

2. Materials. Experimental techniques

Initial materials include tungsten carbide nanopowders produced using DC arc plasma synthesis [3, 4]. The second stage of obtaining α-WC nanoparticles is recovery annealing in hydrogen. Its goal is to control the volume fraction of W_2C, β-WC (WC_{1-x}), W, α-WC particles and free carbon C in a nanopowder charge based on tungsten monocarbide α-WC.

To study the impact that the particle parameters have on the structure and properties of tungsten carbide ceramics, 6 series of powders different in composition were obtained through DC arc plasma synthesis with various average initial particle size (R_0). For the purposes of comparison, this paper involves research into commercial powder α-WC produced by H.C. Starck Company (see Table 1).

Table 1. Impact of the initial particle size and volume fraction of tungsten monocarbide (α-WC) on SPS temperatures and structural parameters of sintered samples (V=25 °C/min, pressure 75 MPa).

Series No.	S (m^2/g)	R_0 (nm)	f (%)	SPS temperatures		Average gain size[2]		Activation energy	Hardness[2]	Fracture toughness[2]
				T_1 (°C)	T_2 (°C)	d_m (μm)	d_a (μm)	Q (kT_m)	H_v (GPa)	K_{1c} ($MPa \cdot m^{1/2}$)
1	8.34	46	83.5	1145	1420	0.1	1-3	5.2	28.0	5.1
2	6.87	55	91.7	1370-1405	1495	0.1	8	5.0	26.0	5.4
3	6.01	63	93.6	1460	1520	0.3	20	4.7	20.0	5.6
4	3.36	113	99.5	1330	1380-1390	2.5-10	17-20	4.1	16.5	6.0
5	5.03	80	100	1425	1505	0.35	1.2-1.3	10.4	34.0	4.3
6	5.27	72	100	1365-1375	1490	0.1-0.15	[3]	10.8	29.0	4.2
7[1]	3.40	112	100	1430	1515	0.2-0.3	[3]	7.7	31.0	4.0

[1] – H.C. Starck powder; [2] – after sintering at 1550°C; [3] – no abnormal grain growth

According to X-ray diffraction analysis, these nanopowders, except for α-WC nanopowders, contained a different number of the following phases: W_2C, β-WC (WC_{1-x}), α-W. As seen from X-ray diffraction patterns for powders with reduced tungsten monocarbide volume fraction (f=83.5-93.6%) clearly show peaks of the primary α-WC phase, as well as β-WC phase (W_xC_{1-x}). α-W tungsten particles in the amount of ~0.5 wt% are identified in powders of Series No.4 at the background level.
Sintering of nanopowders was performed using a sintering plant "Dr. Sinter model SPS-625" in the temperature range from 1400°C to 1950°C without holding. The heating rate (V) ranged from 25 to 2400°C/min. Experiments were carried out at uniaxial compression pressure (P) of 60 and 75 MPa. Sintering took place in 4 Pa vacuum in graphite molds 12 mm in inside diameter.

A dilatometer which is part of a unit "Dr. Sinter model SPS-625" was used to measure effective shrinkage (L_{eff}, mm) under continuous heating (see Fig.1a). To take account of thermal expansion of the "machine-sample" system into effective shrinkage L_{eff} measured with a dilatometer, additional studies into thermal expansion of the system were carried out without samples (empty mold). The above dependencies $L_0(T)$ were then deduced from $L_{eff}(T)$ dependence, and the dependence of shrinkage rate D (Fig. 1b) on the heating temperature was calculated.

Phase composition of samples was studied with "Shimadzu XRD-700" X-ray diffractometer. The chemical composition analysis was performed using "Ultima 2 ICP" atomic emission spectrometer. Vickers hardness (H_v) was measured using "Struers Duramin-5" microhardness tester with a 2 kg load. Fracture toughness K_{IC} was calculated using the Palmqvist method. The intercept method was applied to measure grain size using Jeol JSM-6490 scanning electron microscope.

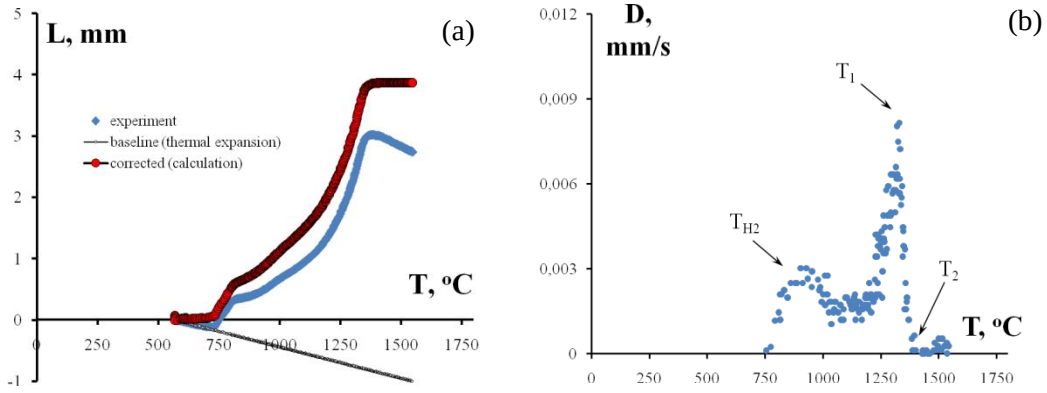

Figure 1. Dependence of shrinkage amount (a) and shrinkage rate (b) on sintering temperature of tungsten carbide nanopowders. Series No.4. Heating rate V=25 °C/min, pressure 75 MPa.

3. Experimental results

3.1. Impact of the initial particle size on tungsten carbide sintering temperature

As seen from Fig.1, D(T) dependence for all the nanopowders under consideration obviously has a three-stage character. Intensity of powder shrinkage is little at an early heating stage. At temperatures below representative temperature T_1, shrinkage rate is growing; with temperature increasing ($T_1<T<T_2$) D(T) value declines rapidly, and at $T\sim T_2$ shrinkage of sintered powders stops.

Data analysis presented in Table 1 proves that representative temperatures T_1 and T_2 depend on the initial particle size: with compositions characterized by low α-WC monocarbide volume fraction (f=83.5-93.6%) increase in the initial size of particles R_0 from 46 nm to 63 nm results in T_1 growing from 1145 °C to 1460 °C and T_2 growing from 1420 °C to 1520 °C. For powders with initial particle size R_0=113 nm and f=99.5%, temperature values are T_1=1330°C and T_2=1380-1390°C (see Table 1).

Thus, it may be claimed that should SPS nanopowders be added up with second-phase particles, nonmonotonic dependence of representative sintering temperatures T_1 and T_2 on the initial particle size R_0 is observed (see Table 1).

During sintering of nanopowders of Series 5-7 (volume fraction for tungsten monocarbide close to 100%), increase in the initial particle size R_0 from 72 nm to 112 nm leads to a monotonic increase in T_1 from 1365-1375°C to 1430°C and insignificant rise in T_2 from 1490°C to 1515°C.

3.2. Impact of nanopowder composition on parameters of the structure formed

Electron microscopic studies prove that abnormal grain growth is observed in the structure of the material sintered from nanopowders added up with second-phase particles (volume fraction of tungsten monocarbide f=83.5-99.5%). After heating to T=1460-1550°C, an inhomogeneous consertal structure is formed with average size of abnormal grains d_a (from 3 to 20 μm) being an order of magnitude bigger than the average size of grains in a matrix d_m (~0.1-0.3 μm) (see Table 1). It is notable that in case of abnormal growth, pores are mainly found along the boundaries of abnormally coarse tungsten carbide grains. With sintering temperature rising to 1700°C, a uniform coarse-grained structure is formed. In this case pores are found both along the boundaries and in the grain boundaries of the sintered material. Analysis of the data presented in Table 1 shows that with tungsten monocarbide volume fraction rising from 83.5 to 99.5%, the average size of abnormally coarse grains d_a is growing from 1-3 to 17-20 μm.

X-ray diffraction analysis illustrates that abnormally coarse grains are W_2C particles. The volume fraction of W_2C particles in sintered ceramics ranges from 2.4 to 10.7% depending on the initial volume fraction of tungsten monocarbide and sintering temperature. The volume fraction of W_2C particles (f_{W2C}) in ceramic samples of Series No.3 (f = 93.6%) and Series No. 4 (f = 99.5%) approximates ~24.4% and ~5.2%, respectively (sintering temperature 1500°C, heating rate V=25°C/min).

For ceramics of Series No.5 obtained through sintering of nanopowders, the volume fraction of tungsten monocarbide in which according to X-ray diffraction analysis constitutes 100%, W_2C particles are identified in the amount ~9.9% (sintering temperature 1500°C, heating rate V=25°C/min). This result brings about the conclusion that the initial volume fraction of the second-phase particles acting as sort of "nuclei's" ("points of grain growth") for abnormally coarse grains is small and lies within the experimental error range permissible for X-ray diffraction analysis.

Note should be taken of no correlation between the volume fraction of nonstoichiometric-phase particles (1-f) and volume fraction of newly formed W_2C particles: in ceramic samples of Series No.3 (f=93.6%), Series No.4 (f=99.5%), and Series No.5 (f~100%) sintered at 1500°C, the volume fraction of W_2C particles is f_{W2C} = 24.4%, 5.2%, and 9.9% respectively. Similar results were achieved while studying ceramics sintered at other temperatures and heating rates. In our opinion the above proves that not all nonstoichiometric-phase particles (W_2C, β-WC (WC_{1-x}), α-W) are "nuclei's" for abnormally coarse W_2C grains while sintering α-WC ceramics. (The nature of "nuclei's" for abnormally coarse grains will be discussed below.)

Research into the structure of samples sintered from nanopowders of Series No.6-7 (volume fracture of tungsten monocarbide is 100%) shows that these materials are characterized by normal grain growth and monomodal grain size distribution, although the distribution bell is rather wide.

The average grain size for samples sintered at 1400 and 1800°C is 90 nm and 350 nm respectively. All the materials under consideration are characterized by active grain growth at temperatures above 1800°C which led to the formation of an UFG structure (average grain size is 300-400 nm).

4. Analysis of experimental data

4.1 Calculation of sintering activation energy

As noted above, dependencies of the degree of shrinkage (L, mm) and shrinkage rate (D, mm/s) on temperature and heating time are considered primary data during SPS of tungsten carbide. The procedure of converting L(T) dependence into compression schedules ρ/ρ_{th}-T is specified in [9, 10] (ρ_{th}=15.77 g/cm^3 being a theoretical density of tungsten monocarbide). ρ/ρ_{th}(T) dependencies have a three-stage nature typical for compression curves during sintering of powder materials. Our further analysis of ρ/ρ_{th}(T) dependencies shall be limited to considering the stage of intensive compression (temperature range $T_1<T<T_2$ shown on Fig.1b).

Activation energy Q of the compression process may be determined by the slope angle of ρ/ρ_{th}(T) dependence (presented in double logarithmic coordinates) on reciprocal temperature T_m/T: $\ln(\ln[(\rho/\rho_{th})/(1-\rho/\rho_{th})]) - T_m/T$ (for more detail see [9, 10]). (T_m=3143 K is the melting temperature for tungsten monocarbide).

Table 1 shows the values of the sintering activation energy Q calculated for compositions with various volume fracture of monocarbide α-WC. In samples of Series No.1-4, the volume fraction of α-WC in which is under 100%, the values of the sintering activation energy within the sintering temperature range T= 1150-1550 °C is Q=107-135 kJ/mol (~4.1-5.2 kT_m), which agrees well with the data obtained in [2] within the same temperature range of 1050-1200 °C during SPS of tungsten carbide nanopowders amid intensive grain boundary (GB) migration: Q =103.5 kJ/mol (~4 kT_m).

Note shall be taken that the obtained values of Q are much lower than the values of the activation energy for GB diffusion Q_b of carbon ^{14}C in coarse-grained tungsten carbide obtained through hot pressing (Q_b=367 kJ/mol ~14 kT_m [11]), as well as the values of the activation energy for ^{14}C diffusion provided in [12] (Q_b=300 kJ/mol ~11.4 kT_m) и в [13] (Q_b=240 kJ/mol ~9.1 kT_m).

In samples of Series No.6-7 (100% α-WC), average values of the Q appear to be considerably higher (7.7-10.8 kT_m~ 201-282 kJ/mol) and better comply with the above reported value [11-13].

Thus, data provided in Table 1 show that two types of behavior are observed during WC sintering: sintering under abnormally low activation energy values and sintering under activation energy corresponding to the equilibrium values of the activation energy for GB diffusion Q_b.

It should be emphasized that after sintering materials of all the above types significantly differ in structure: samples of type 1 materials (sample of Series No.1-4) are characterized by an inhomogeneous structure containing abnormally coarse grains, while samples of type 2 materials (samples of Series No.6-7) form a predominantly homogeneous UFG structure[1].

4.2 Impact of the average initial powder particle size and volume fraction of tungsten monocarbide on the grain growth and WC ceramics density

Let us consider the impact that nonstoichiometric-phase particles of W_2C, β-WC (W_xC_{1-x}) carbides and pure tungsten (α-W) have on sintering of tungsten carbide. Some of these nonstoichiometric-phase particles may act as sort of 'nuclei's' for abnormally coarse grains. (Further, for the sake of brevity, we shall call these particles 'active phase particles').

Let us assume that the typical size to which on average an abnormally growing 'active phase particle' may grow is determined by the distance to another such particle λ^*. Based on microstructural data, it is possible to roughly estimate the volume fraction of such 'active phase particles'. Let us take a simple formula: $\lambda^* = R\sqrt[3]{f_r}$, where f_r and R stand for volume fraction and size of 'active phase particles' respectively. Assuming that λ^* value corresponds to half the size of abnormal grains d_m ($\lambda^*=d_m/2$) and by substituting values R_0=46-113 nm and d_m=3-17 μm (see Table 1) into the equation for λ^*, we shall find that the volume faction of active phase particles' is $f_r \sim 3\cdot10^{-5}$-$3\cdot10^{-4}$%. This value is much smaller than the values of the nonstoichiometric phase volume fraction in samples of Series No.1-4 (from 0.5 to 16.5%) measured with the help of X-ray diffraction analysis. The obtained results also count in favor of the above made assumption that not all nonstoichiometric-phase particles (W_2C, β-WC (W_xC_{1-x}), α-W) are 'active'.

It is crucial to note that the volume fraction of W_2C particles in sintered ceramics is rather high (10-25%), while the volume fraction of W_2C particles in the original powder is below the resolving power of the X-ray diffraction analysis (less than 1%). This means that the SPS process is characterized by 'transformation' of the original 'active phase particles' into W_2C particles which grow rapidly on further heating. Since the experiment shows simultaneous growth in W_2C volume fraction and size (size of abnormally coarse grains), it becomes obvious that this process is not a conventional coalescence process.

In our opinion, the most likely candidate to act as active phase particles may be particles of α-W metal tungsten in which carbon diffusion at specified sintering temperatures (1300-1500°C) is rather intense (parameters of volume carbon diffusion in monocrystals α-W: D_{v0}=3.0 cm^2/s, Q_v=247 kJ/mol ~ 8 kT_m [12]), whereas α-W at elevated temperatures has a high tendency to W_2C carbide formation [14].

We shall note that W_2C phase cannot act as an 'active phase'. This is due to the fact that the volume fraction of W_2C particles in sintered ceramics is much greater than the volume fraction of W_2C particles of the initial powder. This means that the process of splitting the main phase α-WC into W_2C and α-W tungsten ($2WC \rightarrow W_2C + 2W$)[2] shall take place during the SPS process. Such methods as X-ray diffraction analysis and electron microscopy have not detected α-W in the structure of sintered ceramics.

[1] Exception to the above are ceramic samples sintered from nanopowders of Series No.5 in which W_2C particles were discovered and consequently slight abnormal grain growth was detected: the average size of abnormal grains is d_a=1.2-1.3 μm, while the average size of 'matrix' grains is d_m=0.35 μm.

[2] Chances of α-WC particles disintegration during SPS are beyond the scope of this research. Slight W_2C particle formation (under 5%) in ceramics sintered from nanopowders that entirely consist of α-WC tungsten monocarbide was detected only under such simultaneous conditions as extremely high heating rates (1500 °C/min and more) and high sintering temperatures (1720 °C and more). Since such sintering modes are beyond the considered temperature range and sintering rate range, we shall neglect the impact of this factor of the processes discussed.

The hypothesis about the role of tungsten is supported by the results of research [15] into sintering of tungsten carbide with additions of pure tungsten and carbon (pure WC, WC+0.5%W, WC+0.4%C, WC+0.5%W+0.4%C). In [15] shows that with 0.5% α-W particles, the fine structure of a sintered sample accommodates abnormally coarse grains of elongated shape, while a coarse equiaxed structure is formed by sintering other systems.

Summarizing the analysis results it may be concluded that big distance between 'active phase particles' λ^* (the role of which is presumably played by tungsten particles) leads to the fact that with the reduction in the total volume fraction of nonstoichiometric phase the size of abnormally coarse grains d_m is growing.

4.3 Effect of accelerated sintering during abnormal grain growth

Let us consider the issue related to the reasons for lowering the optimal sintering temperature and the reasons why low sintering activation energy values occur in materials with abnormal grain growth.

In our opinion, the said effects may be related to some changes in the parameters of GB diffusion due to intense grain growth in such materials.

In accordance with the concepts of the non-equilibrium GB theory [16, 17], the activation energy of GB diffusion Q_b depends on the degree of grain boundary non-equilibrium, which in turn is determined by the density of defects introduced into GB: orientational misfit dislocations (OMD) with Burgers vector Δb and density ρ_b, as well as products of their delocalization such as a tangential component of delocalized OMD with Burgers vector density w_t. As shown in [16, 18], in case of abnormal grain growth when GB migrating at high speed absorb lattice dislocations distributed in grains, the value of non-equilibrium GB diffusion D^*_b is exponentially dependent on the density of lattice dislocations and grain boundaries migration rate: $D^*_b=D_b\exp(g_1(\rho_v V_m)^n)$, where D_b stands for the diffusion coefficient in equilibrium GB, ρ_v is the density of lattice dislocations, V_m is the GB migration rate, g_1 is a numerical parameter that depends on the thermodynamic properties of the material, n=0.25, 0.5 is a numerical coefficient that depends on what types of defects dominate within grain boundaries: OMD (n=0.25) or tangential components of delocalized dislocations (n=0.5).

The results show an important practical conclusion regarding the impact of the GB migration on the process of SPS of UFG tungsten carbide ceramics. To ensure tungsten carbide sintering at a reduced temperature, it is necessary to optimize its phase composition and sintering modes so as to provide sufficiently 'fast' migration of GB while heating. However, it should be borne in mind that in case of sintering nonstoichiometric powders of tungsten carbide, the abnormal grain growth leads to a decrease in the mechanical properties of sintered samples.

Summary

1. One of the most probable causes of abnormal grain growth during SPS of tungsten carbide is the presence of α-W particles in nanopowders. At elevated temperature tungsten particles react with carbon ($2W + C \rightarrow W_2C$), which results in W_2C particles that are characterized by high migration mobility of boundaries.
2. Rapid migration of GB leads to 'sweeping' by GB of lattice dislocations and reduced activation energy of DB diffusion. This reduces the optimal sintering temperature for tungsten carbide powders. However, materials obtained at low sintering temperatures have low hardness and fracture toughness because of heterogeneity of the grain structure.
3. The effect of reducing the optimal sintering temperature for tungsten carbide powders during SPS is related to the effect of GB diffusion acceleration caused by abnormal grain growth.

Acknowledgements

This research is carried out with the support of the RFBR (Grant No. 15-33-21007) and the Ministry of Education and Science of the Russian Federation.

References

[1] Zhao J, Holland T, Unuvar C, Munir Z A 2009 *International Journal of Refractory Metals and Hard Materials* **27** 130.
[2] Nanda A K, Watabe M, Kurokawa K 2011 *Ceramics International* **37 (7)** 2643-2654.
[3] Krasovskii P V, Malinovskaya O S, Samokhin A V, Blagoveshenskiy Y V, Kazakov V A, Ashmarin A A 2015 *Applied Surface Science* **339** 46.
[4] Isaeva N V, Blagoveshchenskii Y V, Blagoveshchenskaya N V, Mel'nik Y I, Samokhin A V, Alekseev N V, Astashov A G 2014 *Russian Journal of Non-Ferrous Metals* **55 (6)** 585.
[5] Tokita M 2013 *Spark Plasma Sintering (SPS) Method, Systems, and Applications (Chapter 11.2.3)*. In Handbook of Advanced Ceramics (Second Ed.). Ed. Shigeyuki Somiya, Academic Press. 1149.
[6] Orlova A I, Volgutov V Yu, Mikhailov D A, Bykov D M, Skuratov V A, Chuvil'deev V N, Nokhrin A V, Boldin M S, Sakharov N V 2014 *Journal of Nuclear Materials* **446 (1-3)** 232.
[7] Chuvildeev V N, Panov D V, Boldin M S, Nokhrin A V, Blagoveshensky Yu V, Sakharov N V, Shotin S V, Kotkov D N 2015 *Acta Astronautica* **109** 172.
[8] Chuvil'deev V N, Nokhrin A V, Baranov G V, Moskvicheva A V, Boldin M S, Kotkov D N, Sakharov N V, Blagoveshensky Yu V, Shotin S V, Melekhin N V, Belov V Yu 2013 *Nanotechnologies in Russia* **8 (1-2)** 108.
[9] Chuvil'deev V N, Boldin M S, Dyatlova Ya G, Rumyantsev V I, Ordan'yan S S 2015 *Inorganic Materials* **51 (10)** 1047.
[10] Potanina E, Golovkina L, Orlova A, Nokhrin A, Boldin M, Sakharov N 2016 *Journal of Nuclear Materials* **473** 93.
[11] Buhsmer C P, Crayton P H 1971 *Journal of Materials Science* **6 (7)** 981.
[12] Properties, Production and Application of Refractory Compounds. Handbook / Ed. Kosolapova T.Y. 1986 (Moscow: Metallurgiya) 928 p. (in Russian)
[13] Erdelyi G., Beke D.L. Chapter 11 Dislocation and grain boundary diffusion in non-metallic system. In book "Diffusion in Non-Metallic Solids (Part 1)". 1999 (London-Bornstein – Group III Condensed Mater) **33B1** 1.
[14] Kharatyan S L, Chatilyan H A, Arakelyan L H 2008 *Materials Research Bulletin* **43 (4)** 897.
[15] Gubernat A, Rutkowski P, Grabowski G, Zientara D 2014 *International Journal of Refractory Metals and Hard Materials* **43** 193.
[16] Chuvil'deev V N Non-equilibrium grain boundaries in metals. Theory and applications. 2004 (Moscow: Fizmatlit) 304 p. (in Russian)
[17] Chuvil'deev V N, Kopylov V I, Zeiger W 2002 *Annales de Chimie: Science des Materiaux* **27(3)** 55.
[18] Nokhrin A V 2012 *Technical Physics Letters* **38 (7)** 630.